Effect of AlCl$_3$, CH$_3$SO$_3$H on thickness, current efficiency and corrosion properties of brush plated Cr(III) formate urea baths

G. Saravanan, S. Mohan*, R. M. Gnanamuthu and J. Vijayakumar

Brush plating technique was used to deposit trivalent Cr for the first time and effects of AlCl$_3$ and methane sulphonic acid (CH$_3$SO$_3$H) in the trivalent Cr bath was studied. Advantages of brush plated Cr on suitable substrate produced by selective area deposition process with required thickness was investigated. Owing to its portability, flexibility and easy to operate, brush plating has found increasing use in industry. The main applications are for repair and resizing purposes. Brush plated Cr on brass substrate has been investigated using XRD, SEM and AFM. X-ray diffraction analysis revealed that the brush plated Cr(110) was crystalline. Uniform surface coverage of the substrate by granular morphology was observed from SEM and AFM. CH$_3$SO$_3$H increases the hydrogen overpotential on Cr deposition, therefore current efficiency and thickness increased. Cr coated from bath containing both AlCl$_3$ and CH$_3$SO$_3$H have better corrosion resistance due to high charge transfer resistance R_{ct} and very low I_{corr} than Cr(III) bath without these additives.

Keywords: Coatings, Deposition, Brush plated, Trivalent Cr, Corrosion resistance, Methane sulphonic acid (CH$_3$SO$_3$H)

Introduction

Cr is used in industry because of its excellent wear, corrosion, erosion resistance and attractive appearance.[1,2] The main advantage of Cr(III) plating bath in comparison with a Cr(VI) bath is that Cr^{3+} ions are non-toxic environmentally benign.[3] However, it is almost impossible to deposit the Cr coating from a simple aqueous Cr(III) solution due to a very stable [Cr(H$_2$O)$_6$]$^{3+}$ complex.[4] According to the published data[5] the slow deposition rate in Cr(III) chloride electrolyte is related to the appearance of very stable μ-hydroxo-bridged oligomeric species of Cr(III). To destabilise the strong hexa-aqua Cr(III) complex. Some of the complexing agents (glycine, urea, formic acid, acetate, sodium citrate, DL aspartic acid, etc.) may be used.[6–10] The most important fact is that Cr(III) does not oxidise organic compounds. Although the pH in the bulk of the electrolyte may be about 1–2, the diffusion layer pH can reach 4–5. At this pH coordinated water molecules may be converted to OH$^-$ groups, which lead to the formation of μ-hydroxo-bridged species. This reaction may leads to formation of large molecules where the Cr atoms are linked with OH$^-$ groups (olated compounds). This is the cause of losses in both the deposition rate and the quality of Cr deposit. The coordinated water molecules, OH$^-$ groups, or other ligands may be replaced by anions in the solution. Anion that easily enter into the coordinated sphere and displace OH$^-$ groups can effectively prevent olation.[11] Some of the organic ligands influence the plating rate and the quality of the coatings due to the formation of Cr(III) active complexes.[12–14] The AlCl$_3$ enhancing the stability of the bath and quality of Cr deposits. It is well known that AlCl$_3$.6H$_2$O will form the hexa-aqua ion [Al(OH$_2$)$_3$]$^{3+}$ in aqueous solution. The aqua Al(III) complexes hydrolyse especially in the region close to the cathode. So the addition of AlCl$_3$ to the electrolyte led to a high rate of deposition, improved the brightness of deposits and stabilised the electrolyte over its lifetime to give more consistent good quality deposits.[8]

The purpose of this work was to examine the effect of AlCl$_3$, and CH$_3$SO$_3$H[15] on the quality and current efficiency of Cr deposit and to find optimum bath composition and plating conditions for Cr deposition from Cr(III) bath containing formic acid and urea as a complexing agents. Reference 15 shows the effect of methane sulphuric acid on hexavalent Cr plating where as the authors' work was to study the effect of methane sulphonic acid on trivalent Cr along with Al chloride. Methane sulphonic acid accelerates the deposition of Cr and increases its current efficiency because of higher hydrogen overpotential.
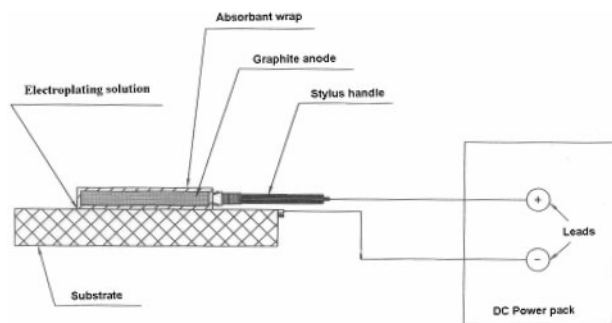
Experimental

Electrolyte and brush plating

Electrodeposition of Cr was carried out from a trivalent Cr formate urea plain bath containing 0·8M CrCl$_3$.6 H$_2$O, 0·5M NH$_4$Cl, 0·5M NaCl, 0·3M B(OH)$_3$, 200 mL

Central electrochemical research institute, Karaikudi, 630006, India

*Corresponding author, email sanjnamohan@yahoo.com

1 Schematic of brush electroplating process

CH_3OH and additionally 7·5 mL $HCOOH$ and 2M $(NH_2)_2CO$ as complexing agents. The effect of $AlCl_3$ and CH_3SO_3H on thickness, current efficiency, structure and corrosion measurement were studied. The pH of these solutions was adjusted to 1–2 ± 0.2 by addition of HCl or KOH. Brush plating equipment includes power packs, solutions and plating tools, anode covers and auxiliary equipment. Microprocessor controlled selectron power pack model 150 A–40 V was used to transform AC current to DC current. The schematic of the brush plating system is given in Fig. 1. The power packs have two leads, one is connected to the plating tool and the other is connected to the workpiece to be plated. The anode is covered with an absorbent material, which holds the solution. The operator dips the plating tool in the solution and then brushes it against the surface of the workpiece that is to be finished. When the anode touches the work surface a circuit is formed and deposit is produced.

Electrochemical measurements

Electrochemical experiments were performed using an advanced electrochemical system (Princeton Applied Research, USA), model PARSTAT 2273 the experiments were conducted at room temperature. The polarisation curves and AC impedance spectra were obtained in 3·5% NaCl aqueous solution. A three electrode cell was used for electrochemical measurements. The working electrode is the Cr coated by brush plating on mild steel. The counter and reference electrode are a large Pt foil and a saturated calomel electrode (SCE) respectively. Measurement of polarisation

curves was carried out at scan rate of 5 mV s^{-1}, from -0.25 to 0.25 V with respect to open circuit potential. AC impedance spectra were recorded for the frequency range from 100 KHz to 10 mHz with the AC amplitude equal to 5 mV s^{-1}.

Characterisation

The microstructure and surface morphology were carried out by scanning electron microscope (SEM) employing a Hitachi 3000H. Structure characterisation of the deposit was carried out by X-ray diffraction (XRD) using a Phillips diffractometer with Cu K (2·2 kW max.) as source. The surface topography of Cr coating was studied using atomic force microscopy (AFM). The basic study comprised a three-dimensional representation for scanned area of 1×1 µm.

Results and discussion

Effects of $AlCl_3$ and CH_3SO_3H on thickness and current efficiency

Figure 2a and b shows the effect of $AlCl_3$ and CH_3SO_3H on thickness and current efficiency of brush plated Cr from various baths. Thickness and current efficiency of Cr deposit is reached maximum of 17·6 µm and 22·75 at 5 A cm^{-2} in 15 min when bath contains CH_3SO_3H acid than the other baths. So from the results CH_3SO_3H acid alone increases both thickness and current efficiency without $AlCl_3$, This is because CH_3SO_3H increase the hydrogen overpotential on Cr deposition thereby hydrogen evolution is inhibited.[15,16]

## Analysis of SEM

The surface morphology of Cr electrodeposited from the bath with and without $AlCl_3$ and CH_3SO_3H were shown in Fig. 3a–d respectively. Figure 3a shows amorphous smooth with microcracks Cr coating layer and enough carbon is deposited as Cr–C and is incorporated from bath containing $AlCl_3$ as additives.[2] Figure 3b and c are SEM images of Cr coating that contains fine grained nodular deposits with particle size is 1·6 µm from bath containing $AlCl_3 + CH_3SO_3H$ and CH_3SO_3H respectively. Figure 3d shows fine grained nodular deposit of size ~ 2 µm in bath without $AlCl_3$ and CH_3SO_3H.[15]

Figure 3c shows uniform surface covered crack free nodular deposit from bath containing only methane
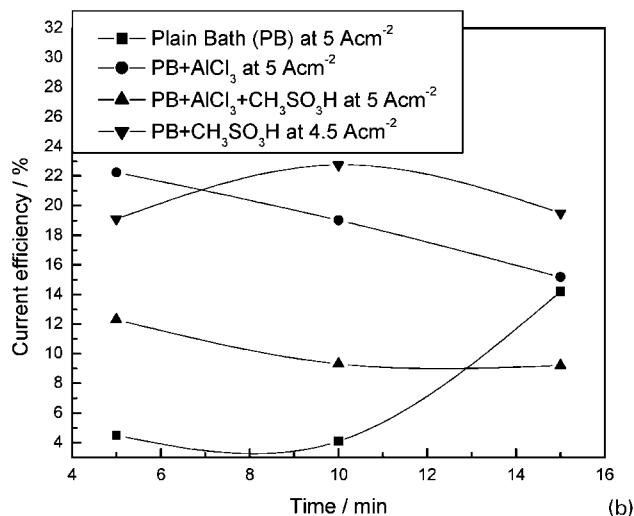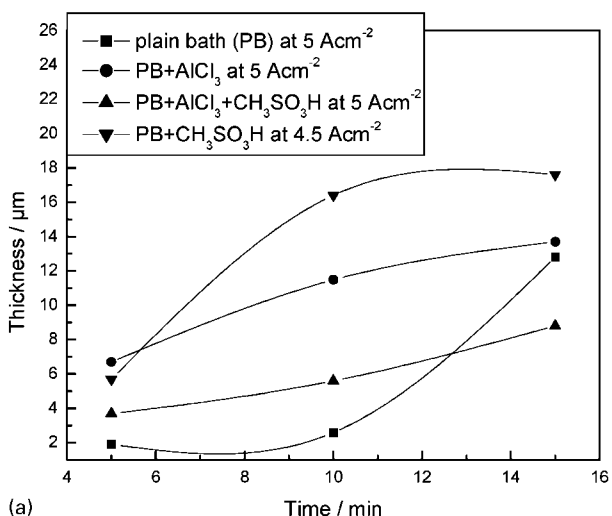
2 Effect of current density on thickness and current efficiency of deposit in various bath compositions
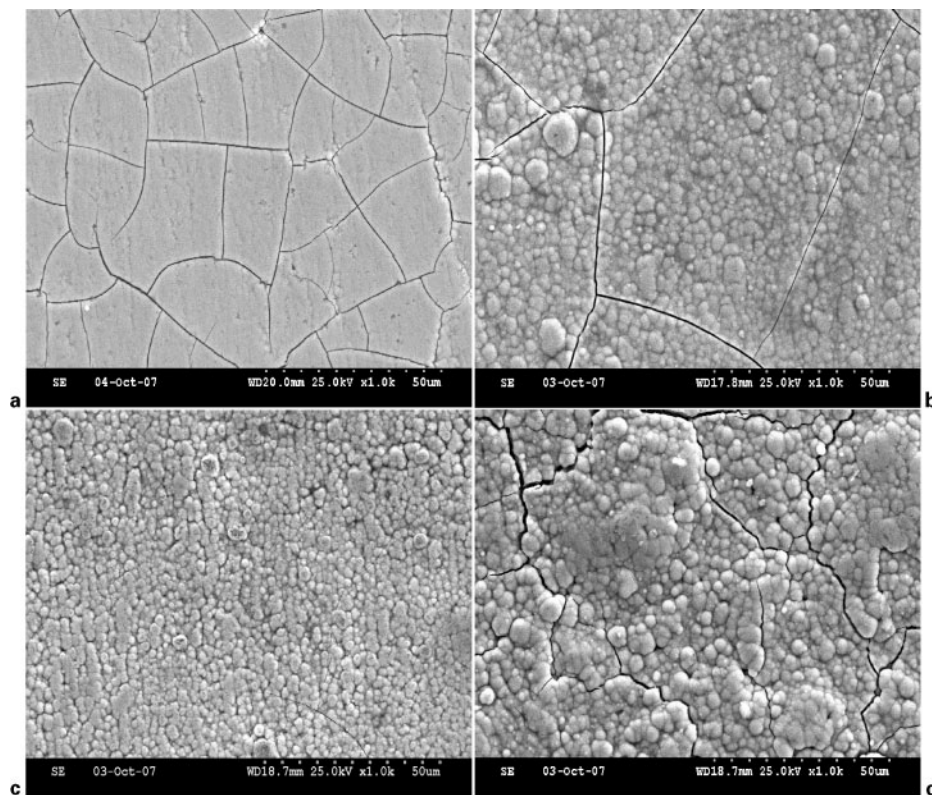
3 Images (SEM) micrographs of brush plated Cr *a* plain bath + AlCl₃, *b* plain bath + AlCl₃ + CH₃SO₃H, *c* plain bath + CH₃SO₃H and *d* plain bath

sulphonic acid as additive. CH_3SO_3H acid increases hydrogen overpotential on Cr electrodeposition and inhibits adsorption of hydrogen gas, so uniform fine grained nodular deposit obtained.

Analysis of AFM

Surface topography of brush plated Cr sample was carried out using AFM. Pictures of AFM scanned over an area of 1×1 μm are shown in Fig. 4. The advantage of AFM is its capacity to probe minute details to the individual grains and intergrain regions. Figure 4*a* shows that deposit consists of grains with few clusters on the entire surface and globule size in the range of 100–300 nm in plain bath with out $AlCl_3$ and CH_3SO_3H. This is because size of crystallites increases with increaseing thickness of coating and agglomerates formed by dispersoids are distinctly seen in the deposits. Figure 4*b* show the deposit consists of many small spherical particles characteristic of bath containing only CH_3SO_3H. The smaller grain size may be conditioned by progressive nucleation during electrode deposition. Nodules are no longer formed and a fine and smooth grained structure is formed. Similar trend is observed in Refs. 8 and 15. From the horizontal cross section analysis, the minimum and maximum globule size was estimated to be in the range of 50–150 nm. Figure 4*c* shows the intermediate grain size and grain size was estimated to be in the range of 120–200 nm from the bath containing $AlCl_3$ and CH_3SO_3H. This is due to the partial agglomerates and nucleation during electrodeposition.

Analysis of XRD

Cr may be electrodeposited in various phases (*α*-, *β*- and *γ*-phases).[17] The phases obtained are dependent on plating conditions. *α*-Cr (Ref. 18) is the most predominant and stable phases, however, *β*-Cr only deposited under certain conditions and converts eventually to *α*-Cr over time or with annealing. The XRD spectra of these Cr deposits are shown in Fig. 5 all the deposits are crystallite and size is <20 nm. The Cr deposited by brush plating consists mainly of *α*-phase (bcc structure) as indicated by the presence of $110(2\theta=44\cdot33)$ and $211(2\theta=81\cdot73)$. However, the peak at $2\theta=64\cdot40$ is attributed to the presence of 200 plane of *γ*- Cr. Similarly, there are four sharp peaks at 2θ 42·29(111), 49·19(200), 72·10(220) and 87·39(311) in XRD patterns. This crystal structure is caused by copper in brass substrate due to small thickness (<16 μm) of deposits. The crystallite sizes of Cr coatings were calculated from the Scherer's equation

$$D = \frac{0\cdot94\lambda}{\beta\cos\theta} \tag{1}$$

where D is the grain size, β is the full width at half maximum (FWHM) of the diffraction peak, λ is the wavelength of the incidental X-ray (1·54 Å), and θ is the diffraction angle. Based on equation (1), the average crystallite sizes were found to be 15·07 nm Cr(110), 14·02 nm Cr(200) and 13·06 nm Cr(211) respectively.

## Potentiotopic polarisation and AC impedance measurements

The potentiodynamic polarisation and AC impedance measurements obtained for the mild steel (A), brush plated Cr in (plain bath + AlCl₃)(B) and brush plated Cr in (plain bath + AlCl₃+CH₃SO₃H)(C) on mild steel in 3·5% w/v NaCl electrolyte are presented in Fig. 6. The equivalent circuit for a corresponding metal which has both anodic and cathodic reaction activation controlled
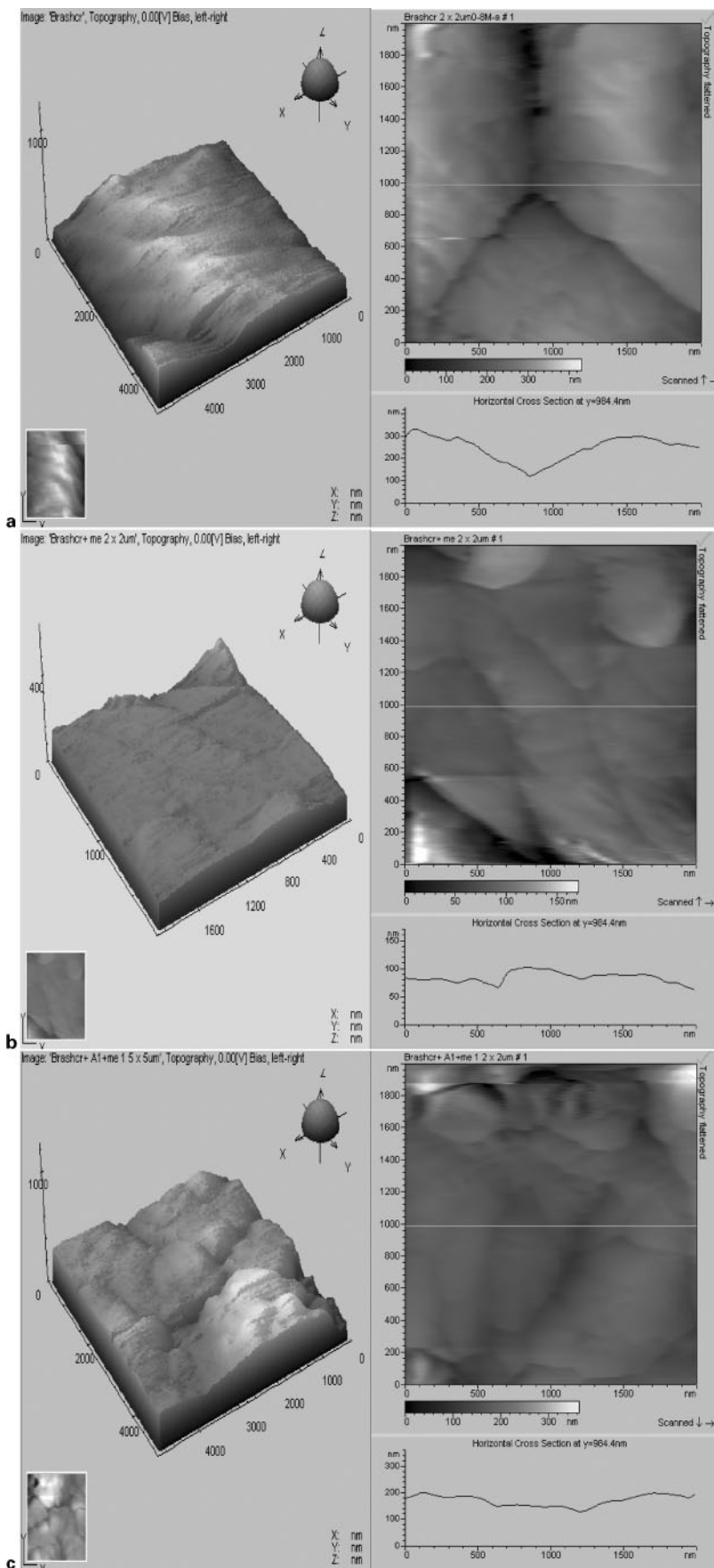
4 Topography (AFM) of brush plated Cr *a* plain bath, *b* plain bath + CH₃SO₃H and *c* plain bath + AlCl₃ + CH₃SO₃H

may be represented as in Fig. 7. The E_{corr} and I_{corr} values have been calculated using the Tafel extrapolation method and they are given in Table 1. There is an

appreciable increase in corrosion resistance for brush plated Cr in (plain bath + AlCl₃ + CH₃SO₃H) (C) and Cr in (plain bath + AlCl₃) (B in Fig. 6) than that of the
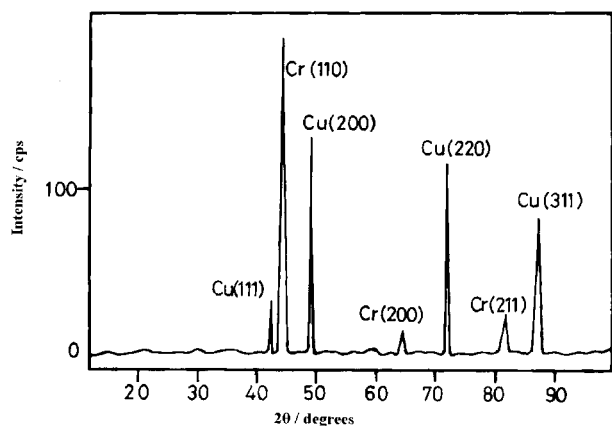
5 X-ray diffraction patterns of brush plated Cr

mild steel (A in Fig. 6). The lower I_{corr} and less negative of E_{corr} signify an improvement in corrosion. The Cr coating serves as an effective barrier to protect the matrix against corrosion attacks. Impedance measurements were made at open circuit potential applying an AC signal of 5 mV s^{-1} in the frequency range from 100 KHz to 10 mHz. The impedance results obtained from bode plots are shown in Table 1 and Fig. 6b. The increased R_{ct} values, decreased C_{dl} values and also it is
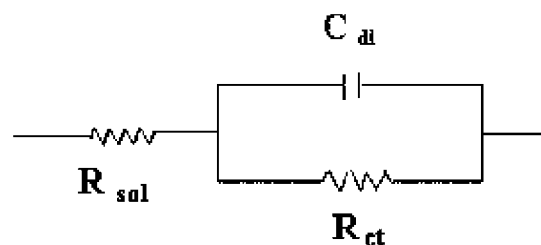

7 Equivalent circuit for corroding metal

observed a more pronounced semicircular region for brush plated Cr in (plain bath + AlCl$_3$ + CH$_3$SO$_3$H) (C) and Cr in (plain bath + AlCl$_3$) (B) than that of the mild steel (A) as shown in Fig. 6.

Conclusions

1. Cr (III) formate urea based electrolyte were developed from which effect of AlCl$_3$ and CH$_3$SO$_3$H were studied. The bath containing CH$_3$SO$_3$H increases both thickness and current efficiency because of higher hydrogen overpotential. Thickness and current efficiency of Cr deposit is reached maximum of 17·6 μm and 22·75 at 5 A cm^{-2} in 15 min.

2. Al chloride enhanced the stability of complex and also increases the quality of deposits. Methane sulphonic
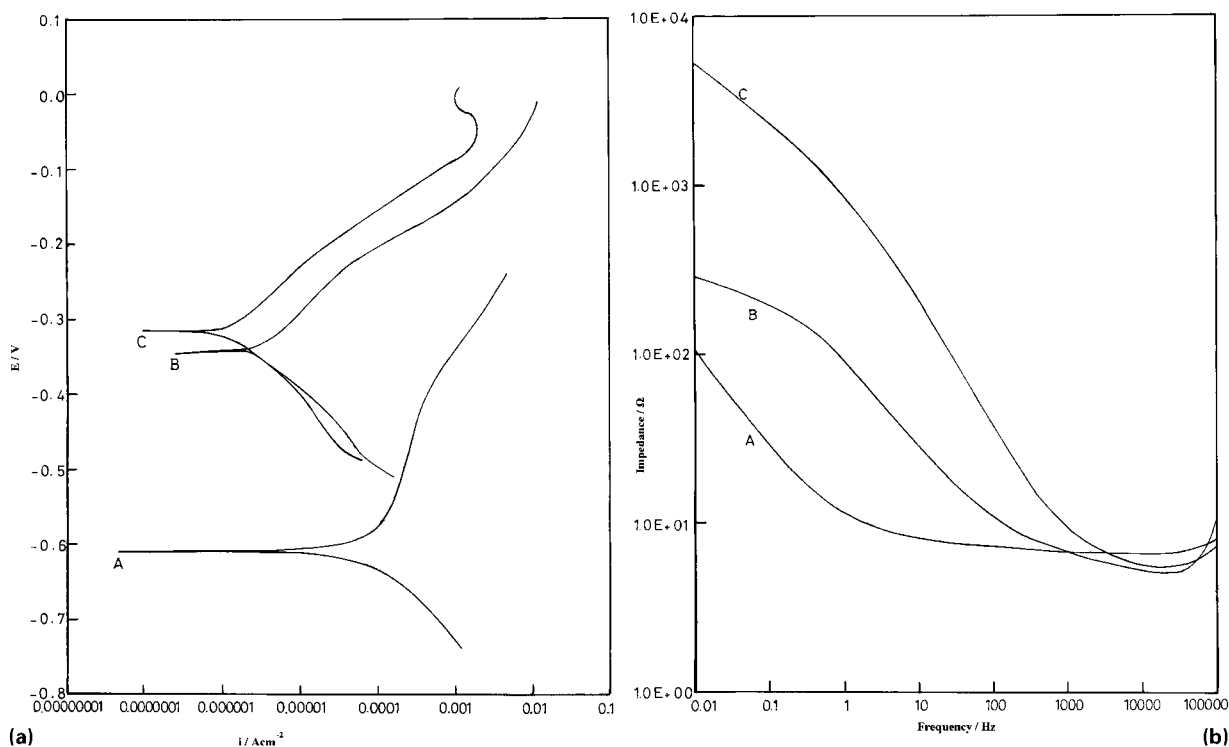
6 *a* polarisation curve and *b* bode plots of (A) MS panel, (B) Cr on MS (plain bath + AlCl$_3$) and (C) Cr on MS (plain bath + AlCl$_3$ and CH$_3$SO$_3$H)

Table 1 Corrosion parameters obtained from polarisation and impedance measurements by bode plots in 3·5% w/v NaCl electrolyte

Sample	E_{corr} versus SCE, mV	b_a, V/decade	b_c, V/decade	I_{corr}, A cm^{-2}	Corrosion rate, mpy	Open circuit potential, V	R_{ct}, Ω cm^2	C_{dl}, F cm^{-2}
MS panel	−0·610	0·250	−0·102	840	85	−0·489	15·1	0·156
Cr on MS (plain bath + AlCl$_3$)	−0·341	0·084	−0·097	26	80	−0·262	255	0·044
Cr on MS (plain bath + AlCl$_3$ and CH$_3$SO$_3$H)	−0·320	0·144	−0·713	4·6	1·4	−0·272	5343	0·021

acid increase the hydrogen overpotential and this leads to increase in thickness, current efficiency and improvement in morphology of deposits.

3. Corrosion measurements shows appreciable increase in corrosion resistance for brush plated Cr in bath containing both $AlCl_3$ and CH_3SO_3H than that of the mild steel (A in Fig. 6).

4. Images of SEM, AFM and XRD of brush plated Cr shows fine grained nodular cracks free and micro crystalline deposit are obtained.

Acknowledgement

References

1. Z. X. Zeng and J. Y. Zhang: *Surf. Coat. Technol.*, 2008, **202**, (12), 2725–2730.
2. K.-S. Nam, K.-H. Lee, S.-C. Kwon, D. Y. Lee and Y.-S. Song: *Mater. Lett.*, 2004, **58**, 3540–3544.
3. S.-C. Kwon, H.-J. Lee, J.-K. Kim, E. Byon ,G. Collins and K. Short: *Surf. Coat. Technol.*, 2007, **201,** (15), 6601–6605.
4. B. Li, A. Lin and F. Gan: *Surf. Coat. Technol.*, 2006, **201**, (6), 2578–2586.
5. S. K. Ibrahim, D. T. Gawne and A. Watson: *Trans. Inst. Met. Finish.*, 1998, **76**, (4), 156–161.
6. S. Surviliene, V. Jasulaitiene, O. Nivinskiene and A. Cesuniene: *Appl. Surf. Sci.*, 2007, **253**, (16), 6738–6743.
7. J.-Y. Hwang: *Plat. Surf. Finish.*, 1991, **78**, (5), 118–124.
8. M. El-Sharif, S. Ma and C. U. Chisholm: *Trans. Inst. Met. Finish.*, 1999, **77**, (4), 139–144.
9. Y. B. Song and D.-T. Chin: *Electrochim. Acta.*, 2002, **48**, (4), 349–356.
10. N. V. Mandich: *Plat. Surf. Finish.*, 1997, **84**, (5), 108–115.
11. C. Barnes, J. J. B. Ward and J. R. House: *Trans. Inst. Metal. Finish.*, 1977, **55**, 73–77.
12. D. Smart, T. E. Such and S. J. Wake: *Trans. Inst. Met. Finish.*, 1983, **61**, 105–110.
13. D. J. Barclay, N. Deeman, T. E. Such and J. M. Vigar: Proc. Conf. Interfinish 80, Kyoto, Japan, October 1980, The Metal Finishing Society of Japan, 79.
14. M. El-Sharif, J. McDougall and C. U. Chisholm: *Trans. Inst. Met. Finish.*, 1999, **77**, (4), 139–144.
15. E. A. Efimov and L.D. Tok: *Protect. Met.*, 2000, **36**, (6), 609–610.
16. B. S. Li, A. Lin, Xu Wu, Y. M. Zhang and F. X. Gan: *J. Alloys Compd*, 2008, **453**, (1–2), 93–101.
17. H. Dasarathy, C. Riley and H. D. Coble: *J. Electrochem. Soc.*, 1994, **141**, 1773–1779.
18. D. Sherwood and B. Emmanuel: *Cryst. Growth Design*, 2006, **6**, 1415–1419.